Hydrate thermal expansivity measurements

Z. Huo, K. T. Miller[1], and E. D. Sloan, Jr.[*]
Center for Hydrate Research
[1]Dept. of Material and Metallurgical Engineering
Colorado School of Mines
Golden, CO 80401

Abstract

It was demonstrated that a minor hydrate lattice parameter change (i.e. 0.5%) may lead to major methane hydrate formation pressure prediction change (i.e. >15% at 100MPa). A hydrate lattice parameter model is the key factor to improving current hydrate predictions. Accurate hydrate thermal expansivity measurements are the first step toward a lattice parameter model.

In this work, we measured both sI and sII hydrate lattice parameters as a function of temperature. It was found that, within experimental error, both sI and sII hydrates had the same thermal expansivities. Two universal lines were developed to express the relative changes in sI and sII lattice parameters as a function of temperature.

Corresponding author: Tel: 303-273-3723, Fax: 303-273-3730, email: esloan@mines.edu

1 Introduction

In the well-known statistical thermodynamic model developed by van der Waals and Platteeuw (1959), it was assumed that there was no hydrate lattice distortion due to either guest type or guest size. However, X-ray diffraction measurements by different researchers (von Stackelberg, 1954 (a, b); Mak and McMullan, 1965; Sargent and Calvert, 1966; McMullan, Jeffrey and Panke, 1970; etc.) had shown that when hydrates were formed from different guest types and guest mixtures, the lattice parameters could be changed substantially. Some existing programs (CSMHYD, Sloan, 1998) have shown that even though the van der Waals and Platteeuw model works very well under certain conditions, it has limitations at high pressures and with uncommon guests.

Ballard (2002) demonstrated that minor lattice parameter changes (i.e. 0.5%) could lead to a significant difference in hydrate formation condition predictions. For methane hydrate, this difference could be at least 15% at high pressures (i.e., >100MPa). The limitations of the van der Waals and Platteeuw model may partially be due to the fact that it did not account for lattice parameter variations for different guests. To modify the original model, Ballard and Sloan (2002a) proposed to account for the lattice parameter changes in the next generation of the hydrate prediction model CSMGem (Ballard, 2002; Ballard and Sloan, 2002a, b).

Unfortunately, existing hydrate lattice parameter measurements were either taken on water-soluble formers, or with errors (i.e. >0.5%) intolerable for accurate

hydrate formation prediction. Systematic measurements on natural gas hydrate lattice parameters were required for natural gas hydrate predictions.

Since natural gas can be a mixture of many components (methane, ethane, propane, …) at any composition, it is impossible to measure the lattice parameter for each production system. The concept was to take limited measurements and model natural gas hydrate lattice parameters based on single or binary guest hydrate formation conditions. In this paper, we measured hydrate thermal expansivities as the first step toward a hydrate lattice parameter model.

As shown in Figure 1, literature data on methane (Gutt, 1999), CO_2 (Ikeda, et al., 1999) and ethylene oxide (Tse & McKinnon, 1987) sI thermal expansivities appeared to follow a general trend with some scatter in the data. Confirmative measurements were required for two purposes: 1) to determine if there was truly a trend and, 2) to determine if this trend applied to other hydrate formers.

The literature data for structure II hydrates are much more uncertain. As shown in Figure 2, it is not clear if the thermal expansivity of sII hydrates varies with guest type. However, the uncertainty may arise from the low accuracy of those measurements. As mentioned by Sargent and Calvert (1966), the accuracy of trimethylene oxide hydrate measurements was ±0.07 Å. As shown in the figure, this error is significant compared to the lattice parameter increase caused by the temperature increase. SII hydrates are of greater concern to the energy industry;

therefore, this work is obliged to quantify sII hydrate lattice parameter with different guests.

2 Apparatus and Experimental Procedures

A Siemens D-500 X-ray diffractometer (donated by Chevron-Texaco) with a cobalt X-ray tube (λ = 1.78897Å) was used in this work. Data collection (MDI DataScan®) and analysis (Jade 5®) software was obtained from Materials Data Inc.. To ensure that the diffractometer was operating properly, the diffractometer alignment was checked every two weeks with a standard sample (SRM 1976®, alumina plate) from the National Institute of Standard and Technology (NIST).

Hydrates were formed in a 20cc pressure cell from ground ice powder. The cell was first cooled by liquid nitrogen; ice powder was then loaded to the cell and sealed. The cell was evacuated at –3°C with temperature controlled by a mono-ethylene glycol bath. Gas of known composition was finally charged to the pressure cell and the temperature was increased slowly to 1°C to allow hydrate formation. This procedure was adopted from Stern et al. (1996).

When gas consumption stopped, as indicated by a stabilized pressure above equilibrium, the hydrate cell was quenched in liquid nitrogen. The samples were then ground to <53 μm powder at 77K. The hydrate powder was finally mixed with 20-30 wt% alumina powder of approximately the same size for use as an internal standard and back loaded into the sample holder. The diffraction side of the sample was sealed

with a 0.05mm thick Kapton® film from Du Pont. Diffraction work was carried out at low temperatures to prevent hydrate dissociation.

Some work (Huo, et al., 2002; Huo, et al., 2003) has indicated that the hydrate lattice parameter is a function of the overall guest-host molar ratio. In this work, a large excess of free gas phase in the cell was always maintained above the hydrate formation equilibrium pressure to ensure a constant hydrate composition so that the lattice parameters were comparable.

During the diffraction experiments, the hydrate sample was cooled with nitrogen boil-off and the temperature was controlled by a temperature and process controller (Omega, cni3233) through a type T thermocouple (Omega, TMTSS-125G, accuracy: ± 0.5K). When stabilized, the temperature fluctuation was within ± 2K. A step size of 0.02^{o} and a counting time of 2 – 3 seconds per step were chosen to get a rapid diffraction pattern. Since condensation occurred on the diffraction surface, ice peaks were always present in each pattern. When diffraction was completed, ice peaks were identified, and hydrate peak positions were adjusted based upon the positions of the internal standard (alumina) peaks. The hydrate lattice parameter was then calculated by a least squares fit using all hydrate peaks.

3 Results

3.1 sI hydrate thermal expansivity measurements

SI hydrates formed from ethane, CO_2, ethane/CO_2, and methane/CO_2 were measured in this work. The results were compared to literature data from both X-ray diffraction (Ikeda, 1999; Gutt, 2000) and neutron diffraction from Oak Ridge National Laboratory (ORNL, Rawn, 2002). As shown in Figure 3, the lattice parameters for different sI hydrates are different, but the increases as a function of temperature are approximately the same in the temperature range from 77 to 220K. This confirmed that there is a general trend in sI hydrate thermal expansivity (i. e. lattice parameter change as a function of temperature). Our CO_2 measurements were compared to the latest neutron diffraction measurements in ORNL (Rawn, 2002). The lattice parameter difference between these two methods was found to be only less than 0.02%, which is approximately the same magnitude as the error in the CO_2 hydrate XRD measurements. Table 1 lists sI hydrate formation conditions and test results.

3.2 sII hydrate thermal expansivity measurements

More sII hydrate thermal expansivities were measured due to industrial interest. As shown in Figure 4, the lattice parameter of various systems such as propane hydrate, black oil hydrate, C_1 + iC_4 hydrate, etc., appeared to follow the same

temperature trend with minor discrepancies. The discrepancies were partially due to the uncertainties in measurements.

The average error in sII hydrate measurements was larger than sI hydrates, especially for systems with substantial amounts of heavy components such as i-butane. When a significant amount of i-butane was present in the gas mixture, low pressures were applied in hydrate formation to avoid liquid hydrocarbon; this usually lead to low ice-hydrate conversion. Low hydrate content in diffraction sample gives low hydrate peak intensities or fewer identifiable peaks.

Green Canyon (GC) gas is a Gulf of Mexico, methane-rich gas mixture with the composition listed in Table 2. Black oil C is a live condensate with the composition listed in Table 3.

Black oil hydrates were formed from water and oil/gas inside a heavily agitated autoclave at high pressure to simulate pipeline conditions. The complexity of the autoclave structure prevented obtaining well-preserved hydrate samples. Upon quenching, hydrates could not be separated from the solid black oil. The presence of ice and black oil in the diffraction sample made black oil measurements less accurate (±0.01Å).

As shown in Figure 4, the results of propane were reproduced and re-measured. No significant difference was observed between two sets (2000 and 2001)

of propane hydrate lattice parameters and thermal expansivities. The propane results were also compared to ORNL neutron measurements (Rawn, 2002). The thermal expansion was found to be the same; however, the lattice parameter differed by approximately 0.06%. Table 4 summarizes sII hydrate thermal expansion results and formation conditions measured in this work.

4 Discussion

4.1 Expressions for sI and sII universal thermal expansivity

The linear thermal expansion coefficient is defined as (Touloukian, et al., 1977, p4a):

$$\alpha = \frac{1}{L}\left(\frac{\partial L}{\partial T}\right)_p \tag{1}$$

where L represents the length, i.e. lattice parameter. If α as a function of T is assumed as:

$$\alpha = a_1 + a_2 T + a_3 T^2 \tag{2}$$

by separation of variables and integration, we get:

$$\begin{aligned} &\frac{L}{L_0} = \exp(a_1(T-T_0) + a_2(T-T_0)^2 + a_3(T-T_0)^3) \qquad or \\ &\frac{L-L_0}{L_0} = \exp(a_1(T-T_0) + a_2(T-T_0)^2 + a_3(T-T_0)^3) - 1 \end{aligned} \tag{3}$$

where L_0 is the lattice parameter at a reference temperature T_0.

To obtain the universal thermal expansion line for sI or sII hydrate, we first estimated such a line based on the data set of CO_2 hydrates for sI and propane

hydrates for sII. The estimated line was then used to calculate the reference lattice parameters for other hydrates. The reference lattice parameter was a hypothetical value at a reference temperature, i.e., T_0 = 273.15K. Once the reference lattice parameter was obtained, the relative lattice parameter change could be calculated for each measurement. The relative lattice parameter change is defined as:

$$y = \frac{a(T) - a_0}{a_0} 100\% \tag{4}$$

where $a(T)$ is the lattice parameter for a certain hydrate at any given temperature, a_0 is the reference lattice parameter of that hydrate. The relative change from the above equation was then compared to the value from the line fit and a difference z was recorded. The universal thermal expansion line was obtained by minimizing the sum of z^2 for all measurements.

For sI hydrates, the following equations express the universal thermal expansivity for different reference temperatures (T_0 = 273.15K):

$$\frac{a(T) - a(T_0)}{a(T_0)} = \exp(9.49\times10^{-5}(T - T_0) + 2.63\times10^{-7}(T - T_0)^2 - 1.46\times10^{-10}(T - T_0)^3 - 1 \tag{5}$$

As shown in Figure 5, equation 5 fits well for both measurements in this work and literature data.

Similarly, sII hydrate relative thermal expansivity is expressed as (T_0 = 273.15K):

$$\frac{a(T)-a(T_0)}{a(T_0)} = \exp(6.45\times10^{-5}(T-T_0)+1.33\times10^{-7}(T-T_0)^2-1.88\times10^{-10}(T-T_0)^3)-1 \quad (6)$$

Again, as shown in Figure 6, within error, such universal lines fit the data very well.

With Eq. (5) and Eq. (6), the relative lattice parameter change (δ) at any given temperature compared to reference temperature (273.15K) may be calculated . The a_0's of any hydrate may then be calculated from the measured lattice parameter a(T) and the relative change:

$$a_0 = a(T_0) = a(T)/(1+\delta) \quad (7)$$

4.2 Structure and guest-host interaction in hydrate thermal expansion

Based on the definition in Eq. (1), the linear thermal expansion coefficient α can be calculated from the derivative of the thermal expansivity expressions. As shown in Figure 7, the thermal expansion of sI and sII hydrates are compatible and both appeared to be much large than that of ice (La Placa and Post 1960; Bril and Tippe, 1967). Tse (1987) attributed the large hydrate thermal expansion mainly to the guest-host interactions, with the distortion of short-range water molecule arrangements (Mak and McMullan, 1965; McMullan and Jeffrey, 1965) as a minor factor.

The guest-host interaction may be the major reason for large thermal expansion of hydrates compared to ice. However, this reason alone may lead to conclusions contradictory to a universal thermal expansion. As indicated by Raman measurements (Sugahara, et al., 2002), the guest-host interaction for ethane sI hydrate is much stronger than that of methane sI hydrate because the former had much smaller compressibility. If guest-host interaction plays a major role in thermal expansion, we would expect different thermal expansivities for different guests.

To rationalize such a contradiction, we propose two types of "guest-host" interactions: one as "normal pressure interaction" and the other as "over-pressure interaction". As shown in Figure 3, the lattice parameter of ethane sI hydrate is significantly larger (by 0.07Å) than that of CO_2 sI hydrate. Assuming that these measurements well represent *in situ* lattice parameters, if the pressure is not very high, the guest-host interactions do not change significantly because the cages are repulsed to accommodate tightly fit guests. Under such conditions, hydrate thermal expansions are not a function of guest type, even though guest-host interaction makes hydrate thermal expansivity dramatically different from that of ice.

Alternatively, when the hydrates are over-pressured to a large extent, with large guests which closely fit within the large cage, a minor reduction in lattice parameter may lead to significantly increased repulsion between guest and host for larger guest molecules, as indicated by Sugahara et al. (2002). This result may occur

because the host cage dimension approaches that of the hard core radius of the larger guest.

5 Conclusions

This work measured both sI and sII hydrate thermal expansivities. Within experimental error, it was found that both sI and sII hydrate thermal expansivities can be expressed by universal lines. The thermal expansion of sI and sII are comparable in the temperature range from 70 to 250K and both were significantly different from ice. A preliminary hypothesis based upon the fit of the guest within the host cage was proposed to explain the universality in hydrate thermal expansions.

6 Acknowledgements

The author thanks Chevron-Texaco for their donation of the Siemens D-500 X-ray diffractometer. The author also thanks BP, Chevron-Texaco, DoE, Haliburton, Petrobras, Phillips and Unocal, for their financial support on this project.

Reference

Ballard, A., Ph. D. Thesis, Colorado School of Mines, Golden, CO, USA, 2002.

Ballard, A. L., and Sloan, E. D., *Proceedings of the Fourth International Conference on Gas Hydrates*, Yokohama, Japan, 19-23 May, p307-314, 2002a.

Ballard, A. & Sloan, E. D., *Fluid Phase Equilibria*, 2002b.

Brill, R., Tippe, A. *Acta Crystallogr*., 23, 343, 1967.

Gutt, C., et al., *Experimental Physik*, to be published (2000).

Huo, Z., Jager, M. D., Miller, K. T., and Sloan, E. D., *Chemical Engineering Science*, 57, 705-713, 2002.

Huo, Z., Hester, K., Miller, K. T., and Sloan, E. D., *AIChE J*., in press (2003).

Ikeda, T., Yamamuro, O., Matsuo, T., Mori, K., Torii, S., Kamiyama, T., Ixumi, F., Ikeda, S., and Mae, S., *J. Phys. Chem. Solids*, 60, 1527-1529, 1999.

La Placa, S., Post, B., Acta Crystallogr., 13, 503, 1960.

Mak, T. C. W. and McMullan, R. K., *J. of Chem. Phys*. 42(8), 2732, 1965.

McMullan, R. & Jeffrey, G. A., *J. of Chemical Physics*, 42(8), 2725 – 2732, 1965.

Mcmullan, R. K., Jeffrey, G. A., and Panke, D., *J. of Chemical Physics*, 53 (9), 3568 – 3577, 1970

Paulling, L., Marsh, R. E., *Proc. Nat. Acad. Sci*. (USA), 38, 1952.

Rawn, C. J., personal communications, 2002.

Sargent, D. F., Calvert, L. D. *J. Phys. Chem*. 70, 2689, 1966.

Shirota, H., Aya, I., Namie, S., and Bollavaram, P., *Proceedings of the Fourth International Conference on Gas Hydrates*, Yokohama, Japan, 19-23 May, p972-977, 2002.

Sloan, E. D., *Clathrate Hydrates of Natural Gases*, 2nd edition, Dekker, New York, 1998.

Stern, L. A., Kirby, S. H., & Durhan, w. B., *Science*, 273: 1843 (1996).

Sugahara, T., Sugahara, K., and Ohgaki, K. *Proceedings of the Fourth International Conference on Gas Hydrates*, Yokohama, Japan, 19-23 May, p608-613, 2002.

Takeya, S., Nagaya, H., *J. Phys. Chem. B*, 104, 668, 2000.

Touloukian, Y. S. et al., *Thermophysical Preperties of Matter, v13: Thermal Expansion: Nonmetallic Solids*, Plenum Publishing Corporation, New York, 1977.

Tse, J. S. & McKinnon, W. R., *J. Phys. Chem*., 91, 4188-4193, 1987.

Tse, J. S., *Journal de Physique*, 48, C1-543 1987.

Van der Waals, J. H. & Platteeuw, J. C., *Advances in Physical Chemistry*, 2, 1-57, 1959.

Von Stackelberg, M., Muller, H. R. *Feste Gashydrate* II, *Z. Electrochem*. 58, 25, 1954a.

Von Stackelberg, M., Jahns, W. *Feste Gashydrate*, *Z. Electrochem*. 58, 162, 1954b.

List of Tables

Table 1 Hydrate formation conditions and measured lattice parameters

Table 2 Composition of Green Canyon Gas

Table 3 Composition of Black Oil C

Table 4 SII hydrate thermal expansion measurements

Table 1 Hydrate formation conditions and measured lattice parameters

C_1/CO_2		C_2		CO_2		C_1/C_2	
Formation:							
C_1	84.94%					C_1	46.67
CO_2	15.06%					C_2	53.33
p	4.14MPa	*p*	4.14MPa	*p*	3.03MPa	p	2.7MPa
T	274.15K	*T*	274.15K	*T*	274.15K	T	274.15K
Diffraction (T in Kelvin):							
T	*a*	*T*	*a*	*T*	*a*	T	a
123	11.853	77	11.8956	77	11.834	133	11.926
83	11.838	98	11.9098	102	11.843	148	11.936
143	11.869	111	11.9189	123	11.855		
153	11.875	123	11.9245	141	11.867		
		133	11.9342	153	11.876		
		145	11.9430	167	11.886		
		157	11.9540	183	11.897		
		173	11.9625	195	11.908		
		188	11.9719	207	11.921		
		203	11.9810				
		217	11.9946				

Table 2 Green Canyon Gas

Component	mole%
C_1	87.24
C_2	7.57
C_3	3.08
iC_4	0.51
nC_4	0.79
iC_5	0.20
nC_5	0.20
N_2	0.40

Table 3 Composition of Black Oil C

Fluid	Wt%	Mole%	Mw
N_2	0.034	0.206	28.0
CO_2	0.002	0.006	44.0
C_1	3.298	35.234	16.0
C_2	0.490	2.792	30.1
C_3	0.271	1.052	44.1
iC_4	0.055	0.163	58.1
nC_4	0.089	0.262	58.1
iC_5	0.053	0.125	72.2
nC_5	0.095	0.226	72.2
C_6	0.656	1.305	84.0
Benzene	0.021	0.045	78.1
Toluene	0.078	0.145	92.2
C_7	1.733	3.095	96.0
C_8	2.769	4.436	107
C_9	3.156	4.471	121
C_{10}	3.284	4.200	134
C_{11}	2.935	3.422	147
C_{12}	2.624	2.794	161
C_{13}	2.704	2.648	175
C_{14}	2.615	2.359	190
C_{15}	2.564	2.133	206
C_{16}	2.311	1.784	222
C_{17}	2.268	1.640	237
C_{18}	2.204	1.505	251
C_{19}	2.108	1.374	263
C_{20}	1.983	1.236	275
C_{21}	1.859	1.095	291
C_{22}	1.803	1.013	305
C_{23}	1.690	0.911	318
C_{24}	1.576	0.816	331
C_{25}	1.538	0.764	345
C_{26}	1.466	0.700	359
C_{27}	1.473	0.675	374
C_{28}	1.451	0.641	388
C_{29}	1.386	0.591	402
$C_{30}+$	45.361	14.136	550
Total	**100**	**100**	

Table 4 sII hydrate thermal expansion measurements

C_3		C_1/C_3		C2/C3		CO_2/C_3		C_1/iC_4		GC gas		Black oil	
Formation conditions													
		C_1	60%	C_2	30%	CO_2	18.20%	C_1	87.60%				
		C_3	40%	C_3	70%	C_3	81.80%	iC_4	12.40%				
p	0.44MPa	*p*	0.5MPa	*p*	0.5MPa	*p*	1.8MPa	*p*	1.3MPa	*p*	8.3MPa	*p*	10MPa
T	274.15K	*T*	274.15K	*T*	274.15K	*T*	274.15K	*T*	273.15K	*T*	277.15K	*T*	276.15K
Diffraction (T in Kelvin)													
T	*a*	*T*	*a*	*T*	*a*	*T*	*a*	*T*	*a*	*T*	*a*	*T*	*a*
77	17.116	77	17.138	143	17.147	208	17.249	153	17.241	184	17.211	213	17.208
161	17.176	243	17.273	113	17.128	222	17.266	165	17.253	200	17.227	178	17.181
191	17.197	226	17.255	188	17.177	193	17.235	175	17.266	212	17.241	133	17.138
206	17.216			221	17.208	181	17.222	188	17.278			143	17.153
230	17.235			238	17.225	143	17.189	198	17.290				
2nd series								208	17.302				
77	17.111							221	17.312				
103	17.131												
121	17.143												
135	17.150												
152	17.160												
165	17.169												
177	17.181												

List of Figures

Figure 1 sI thermal expansivity in literature

Figure 2 sII thermal expansivity in literature

Figure 3 sI hydrate thermal expansivity measurements

Figure 4 sII hydrate thermal expansivity measurements

Figure 5 sI hydrate relative lattice parameter change with temperature

Figure 6 sII hydrate relative lattice parameter change with temperature

Figure 7 Linear thermal expansion coefficient of hydrates and ice

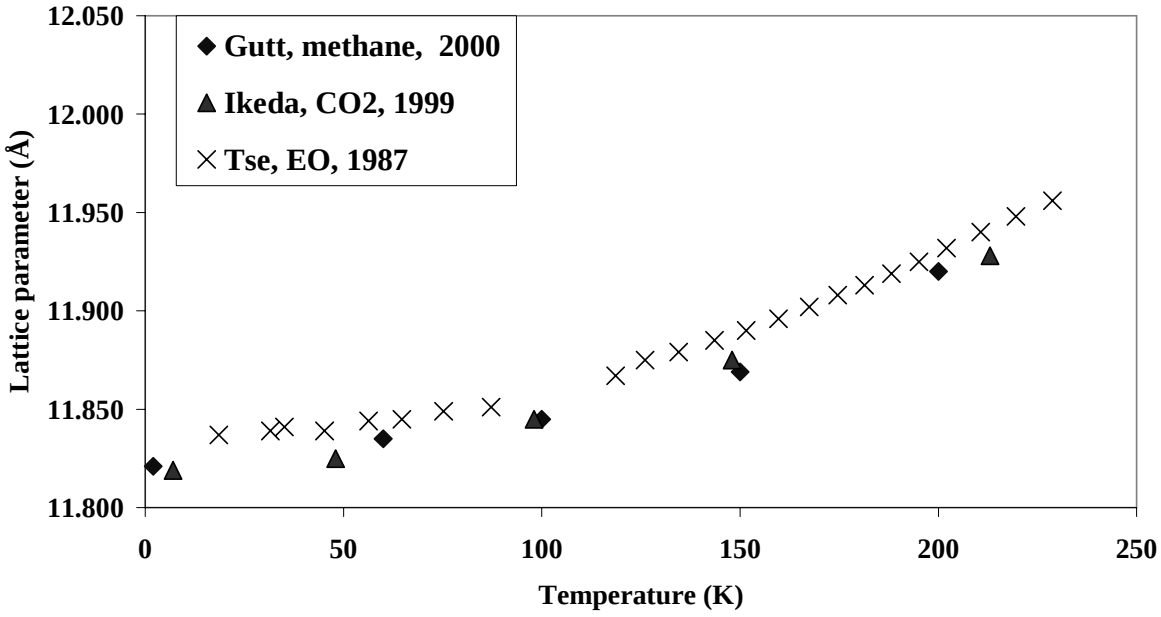

Figure 1 sI thermal expansivity in literature

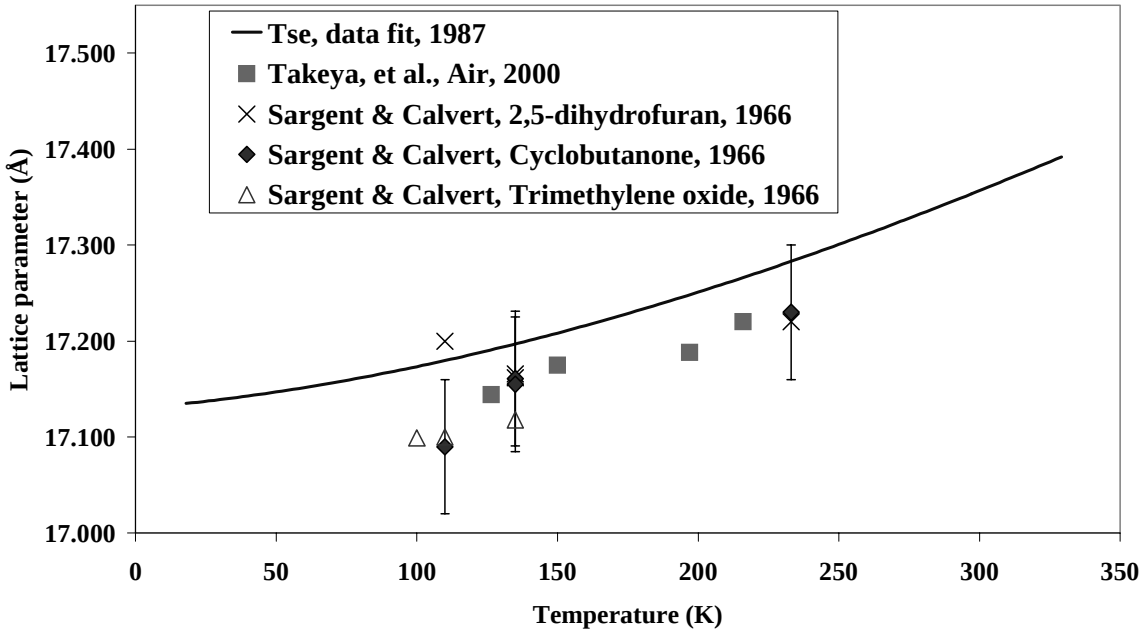

Figure 2 sII thermal expansivity in literature

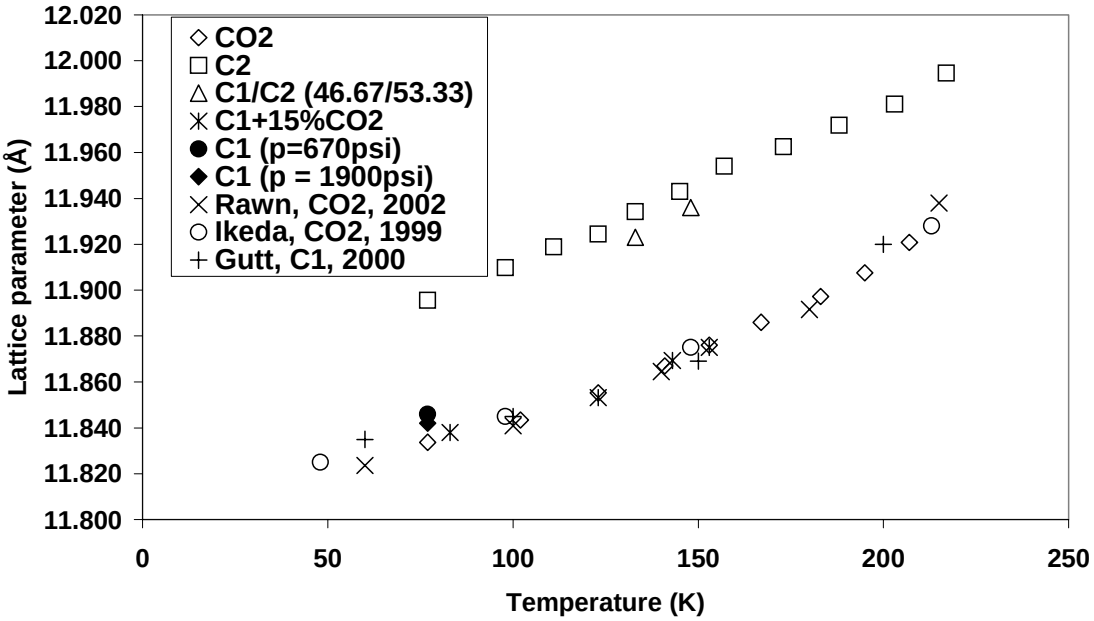

Figure 3 sI hydrate thermal expansivity measurements

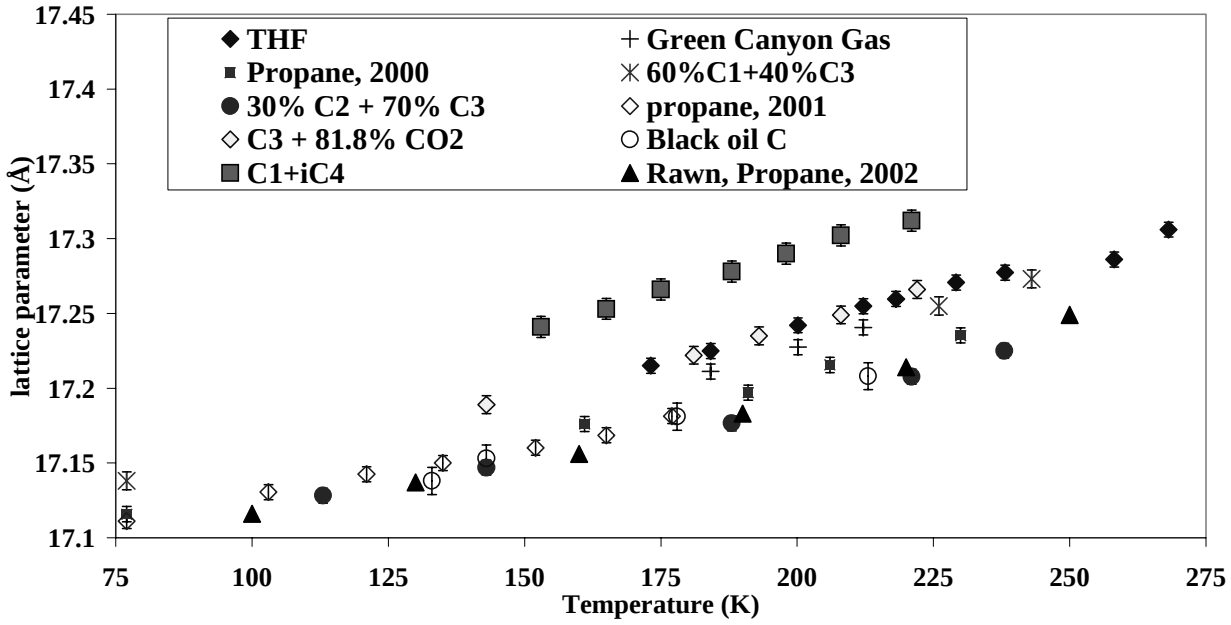

Figure 4 sII hydrate thermal expansivity measurements

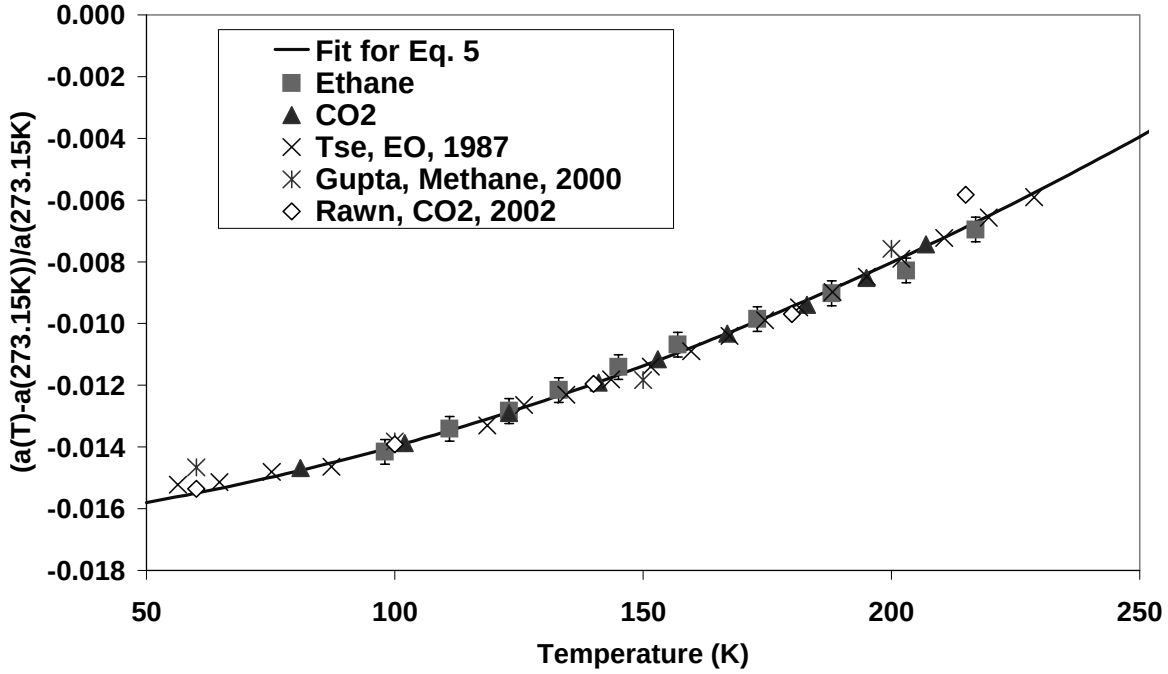

Figure 5 sI hydrate relative lattice parameter change with temperature

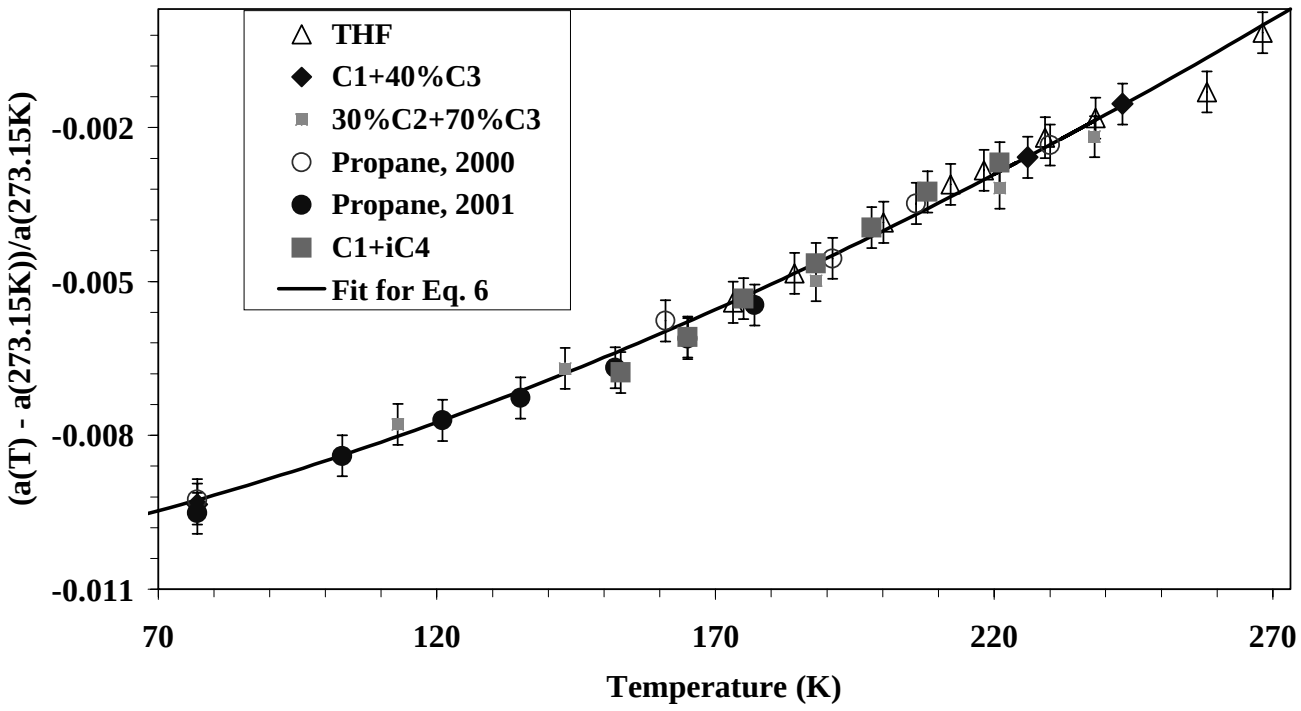

Figure 6 sII hydrate relative lattice parameter change with temperature

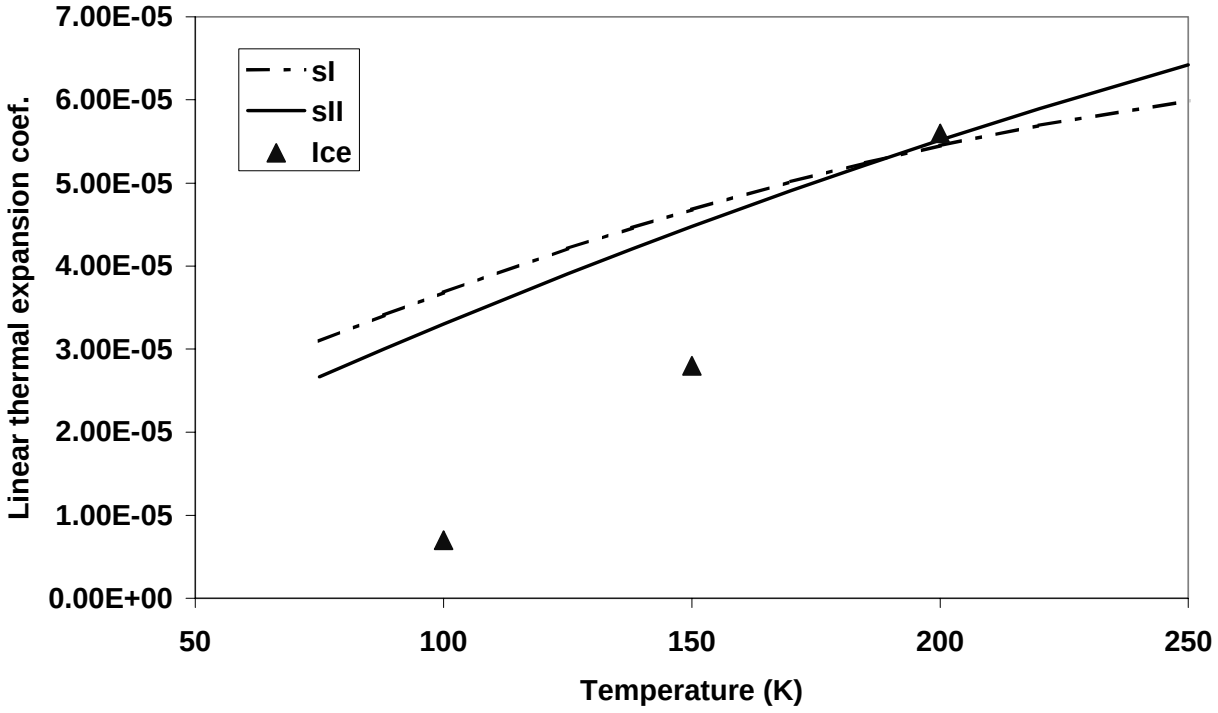

Figure 7 Linear thermal expansion coefficient of hydrates and ice